

## Short-time relaxation at polymeric interfaces

A. Karim, A. Mansour, and G. P. Felcher

*Materials Science Division, Argonne National Laboratory, Argonne, Illinois 60439*

T. P. Russell

*IBM Research Division, Almaden Research Center, San Jose, California 95120*

(Received 6 April 1990; revised manuscript received 27 June 1990)

The interdiffusion of long polymer chains at the interface of two melts has been studied as a function of time by neutron reflection. The time range studied spanned from the time characteristic of the motion of the single segment (Rouse time,  $\tau_e$ ) up to the time at which the center of mass of the whole molecule has moved a radius of gyration (reptation time). At least for  $t > \tau_e$ , the diffusion rate slows down with time until the bulk diffusion rate is reached, in agreement with the current theories for the motion of a polymeric chain in a melt.

The theoretical treatment of the dynamics of a long polymer molecule in a melt has been elegantly developed by de Gennes<sup>1</sup> and Edwards.<sup>2</sup> These authors proposed that a polymer molecule diffuses by moving along its own contour in a reptative manner within the confinements of a hypothetical "tube," which is defined by the entanglements of the molecule with other molecules. The reptation model has been successful in describing the motion of polymer molecules over distances larger than their radius of gyration (or times greater than the reptation time,  $\tau_d$ ). In that region the mean-square displacement of the molecule is predicted to be proportional to time with a diffusion coefficient proportional to  $M^{-2}$  ( $M$  is the molecular weight). These predictions have been extensively confirmed by Kramer and co-workers using forward-recoil spectrometry,<sup>3,4</sup> by Klein and Briscoe, using infrared spectroscopy,<sup>5</sup> and also by secondary-ion mass spectrometry.<sup>6</sup> However, these techniques, with a resolution at best of 100 Å, monitor well the motion of the molecules only for times greater than  $\tau_d$ , since the radius of gyration of a molecule with a typical weight  $M = 230\,000$  is 130 Å.

There is considerably less information available for times shorter than  $\tau_d$ . When we examine diffusion over distances less than the dimensions of the molecule, the constraints due to entanglement between molecules become important. Recently, direct microscopic evidence of a well-defined entanglement distance (or tube diameter) inhibiting the diffusion has been found by Richter *et al.*<sup>7</sup> in a neutron spin-echo experiment. Molecular-dynamics simulation of diffusion of polymer melts by Kremer, Grest, and Carmesin<sup>8</sup> show the presence of two time regimes when the molecular weight exceeds the threshold for entanglement.

We have monitored the diffusive motion of polymers by means of neutron reflection.<sup>9</sup> The quantity examined is the thermally-induced-interdiffusion profile between two layers of polymers deposited on a flat substrate; one of the polymers has been "tagged" by deuterating it. The experiment takes place by bringing a well-collimated neutron beam onto the sample surface at a glancing angle  $\theta$ . The number of neutrons reflected from the sample is recorded as a function of the component of the neutron momentum

perpendicular to the surface,  $k_{z,0} = (2\pi \sin\theta)/\lambda$ , where  $\lambda$  is the neutron wavelength and  $\theta$  the angle of incidence. The reflectivity  $R(k_{z,0})$  is an optical transform of  $b(z)/V(z)$ , the nuclear-scattering amplitude density at a distance  $z$  from the surface of the sample.

The samples investigated were bilayers of normal and deuterated polystyrene (*h*-PS and *d*-PS, respectively), on polished silicon substrates (5-cm diameter, 0.5-cm thickness). The first layer was prepared by coating the substrate with a solution of the polymer in toluene and then spinning it at 2000 rpm to evaporate most of the solvent and produce a uniform film with thickness greater than 1500 Å. The specimen was then annealed at 120°C for 48 h to remove residual solvent and relax the film. The second layer was prepared separately by spin coating a film 600–800-Å thick onto a 5.0×7.0-cm<sup>2</sup> microscope slide. The sides of the slide were scored with a razor blade and the film was floated off onto a pool of deionized water and then transferred to the top of the first layer. The bilayer was dried in vacuum for at least 48 h. Starting from this initial ( $t=0$ ) sample, interdiffusion of the *d*-PS and *h*-PS was achieved by placing the bilayer in a preheated oven under helium, temperature controlled within 0.5°C for a preset time, and then rapidly cooled. The sum of heating and cooling time was small (~45 s) in comparison to the interdiffusion times. The characteristics of the samples used in this study along with their thicknesses are shown in Table I.

The experiments were performed using the reflectometer POSY II at the intense pulsed neutron source at Argonne National Laboratory. Figure 1 shows the neutron reflection spectrum for a typical sample [*h*-PS( $4.75 \times 10^5$ )/*d*-PS( $2.05 \times 10^5$ )] plotted as  $Rk_{z,0}^4$  vs  $k_{z,0}$  before and after annealing for 2 min at 105.5°C. We plot  $Rk_{z,0}^4$  (rather than the reflectivity  $R$ ) because for large  $k_{z,0}$  this quantity becomes a constant whose value depends on the type and the amount of sharp boundaries between the layers of the sample. As can be seen from Fig. 1, even a modest amount of interdiffusion causes a drastic variation of the asymptotic level. Figure 1 also shows that the reflectivity is modulated, as a consequence of the interference between the partial reflections at the boundaries of

TABLE I. Characteristics of the samples along with their thicknesses.

Bilayer specimen <sup>a</sup> surface/bottom layer	Thickness (Å)	Annealing temperature (°C)	Annealing time in minutes diffusion ( $\sigma_t$ in Å)
<i>d</i> -PS( $2.03 \times 10^5$ )/ <i>h</i> -PS( $2.33 \times 10^5$ )	600/2886	130.0	0(10);5(60);49(150);139(220)
<i>h</i> -PS( $2.33 \times 10^5$ )/ <i>d</i> -PS( $5.50 \times 10^5$ )	980/3500	125.0	0(25);10(55);30(70);70(75);150(100);310(125)
<i>h</i> -PS( $2.33 \times 10^5$ )/ <i>d</i> -PS( $5.50 \times 10^5$ )	990/2300	116.3	0(25);10(40);110(65);180(70);2340(145);9840(200)
<i>h</i> -PS( $4.75 \times 10^5$ )/ <i>d</i> -PS( $2.05 \times 10^5$ )	675/1775	116.3	0(15);15(55);30(60);9405(160)
<i>d</i> -PS( $2.03 \times 10^5$ )/ <i>h</i> -PS( $2.33 \times 10^5$ )	600/2000	105.5	0(10);30(30)
		135.0	22(125);53(190)
<i>h</i> -PS( $4.75 \times 10^5$ )/ <i>d</i> -PS( $2.05 \times 10^5$ )	675/1850	105.5	0(10);2(30);62(40);1322(60)
<i>h</i> -PS( $2.33 \times 10^5$ )/ <i>d</i> -PS( $1.03 \times 10^6$ )	790/2600	105.5	0(10);5(25)
<i>h</i> -PS( $2.5 \times 10^6$ )/ <i>d</i> -PS( $2.03 \times 10^5$ )	415/2250	105.5	0(5);5(25)
<i>h</i> -PS( $2.33 \times 10^5$ )/ <i>d</i> -PS( $1.03 \times 10^6$ )	790/3000	100.0	0(10);10(25)

<sup>a</sup>Letter designates the hydrogen isotope of the PS; whereas the number following is the weight-average molecular weight.

each layer. The modulation periods do not shift after annealing, which means that the thermal treatment does not change the layer thickness whose best fitted values are included in Table I. The only parameter to fit the annealed data in Fig. 1 was the thickness of the interface: In this the density profile was assumed to have, somewhat arbitrarily, the form of an error function.

Table I gives a compendium of the experimental root-mean-square thicknesses,  $\sigma_t = \langle z^2 \rangle^{1/2}$ , which are graphi-

cally presented in Fig. 2. Although the samples were, in reality, annealed at different temperatures, we reduced the annealing time to a reference temperature, by using an empirical relation proposed by Williams, Landel, and Ferry (WLF).<sup>10</sup> According to WLF, the relaxation of a polymer as measured at different temperatures occurs in a time  $t$  multiplied by a “shift factor”  $a_T$ . For high-molecular-weight polystyrene ( $M > 10^5$ )  $a_T$  is<sup>11</sup>

$$\log_{10} a_T = \frac{-9.06(T - 120)}{69.8 + (T - 120)} \quad (1)$$

to bring the data to a reference temperature of 120 °C, provided that  $T$  is within 50 °C of the reference temperature. As seen in Fig. 2, the data points from nine different samples fall on a smooth curve over six decades of the reduced-time variable, the main discrepancies being between different samples.

The root-mean-square thicknesses  $\sigma$  presented in Fig. 2

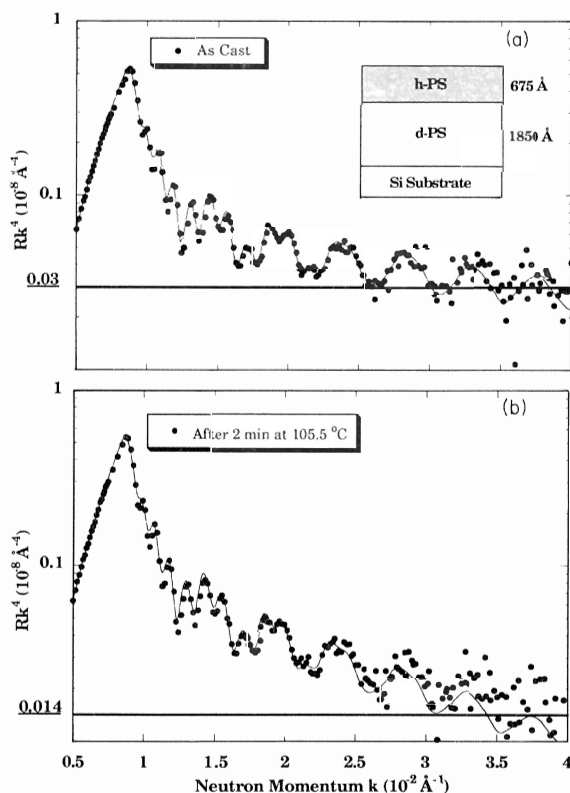


FIG. 1.  $R(k_z)k_z^4$  as a function of  $k_{z,0}$  for a bilayered sample of *h*-PS ( $M_w = 475\,000$ ) on top of *d*-PS ( $M_w = 205\,000$ ) (a) before heating and (b) after heating at 105.5 °C for 2 min. The solid circles are the experimental data whereas the solid lines were calculated using a bilayer model with an error function describing the concentration profile between the upper and lower layers.

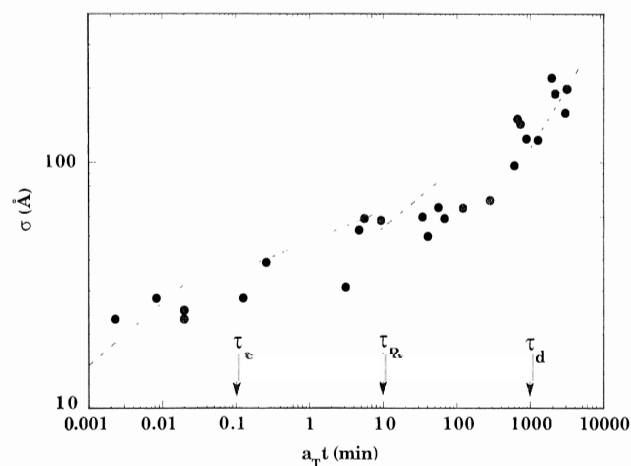


FIG. 2. Root-mean-square halfwidth  $\sigma$  as a function of reduced time  $a_T t$  at a reference temperature of 120 °C. The arrows indicate the Rouse relaxation time for the molecule between entanglement points  $\tau_e$ , the Rouse relaxation time for the whole molecule  $\tau_R$ , and the reptation time  $\tau_d$ . The dashed lines are the calculated values for the displacements in different regimes, according to Eqs. (6a)–(6d), with parameters not adjustable, but prefixed as explained in the text.

have been corrected for the interface "thickness"  $\sigma_0$  of the as-prepared samples. The correction was done quadratically, assuming the two quantities to be statistically independent, i.e.,  $\sigma^2 = \sigma_l^2 - \sigma_0^2$ . A finite value of  $\sigma_0$  does not necessarily mean that interdiffusion has occurred during the sample preparation. The reflectivity measures the scattering-amplitude density averaged on a plane parallel to the surface ( $z = \text{const}$ ), over an area with linear dimensions on the order of the neutron's coherence length. The thickness of an interface might be caused by diffusion, roughness, or short-period wavyness resulting from the film preparation. The accuracy by which the root-mean-square thickness is determined<sup>12</sup> from this is approximately 5 Å, becoming rapidly worse for  $\sigma > 200$  Å.

The arrows in Fig. 2 indicate the positions of the characteristic physical times for these polymers  $\tau_e$ ,  $\tau_d$ , and  $\tau_R$ . The Rouse time  $\tau_e$  is defined<sup>2</sup> as the time at which the segmental displacement becomes comparable to the tube diameter; it corresponds to a segment with molecular weight  $\approx 18000$  for polystyrene (PS):<sup>13</sup>

$$\tau_e \approx \frac{\pi a^6}{36 N^2 b^4 D^*} \quad (2)$$

where  $D^*$  is the self- or bulk-diffusion coefficient of the molecule,  $N$  is the degree of polymerization,  $a$  is the tube diameter, and  $b$  is the statistical segment length of the polymer. The reptation time  $\tau_d$  is the time<sup>2</sup> for complete disengagement of a molecule from its initial tube:

$$\tau_d = \frac{N b^2}{3 \pi^2 D^*} \quad (3)$$

Between these two limits, the Rouse relaxation time  $\tau_R$  indicates the time in which the motion of the single segments become coordinated over the entire length of the chain:<sup>2</sup>

$$\tau_R = \frac{a^2}{9 \pi^2 D^*} \quad (4)$$

Some of the quantities appearing in Eqs. (2)–(4) are well determined experimentally. From step-strain response of PS melts by infrared dichroism,<sup>14</sup>  $\tau_e = 5.6$  s at 120 °C (for a molecular weight  $M_w = 233000$ ,  $N = 2240$ ). The statistical segment length for styrene<sup>1</sup> is 6.7 Å.  $D^*$  is a function of the molecular weight ( $D^* = D_0/M^2$ ) and of temperature [cf. Eq. (1)]: for  $M = 233000$  and  $T = 120$  °C,  $D^* = 5.45 \times 10^{-18}$  cm<sup>2</sup>/s has been determined by forward recoil spectrometry measurement.<sup>3,4</sup> These numerical values define not only the positions of the characteristic relaxation times, but also define the diameter of the tube ( $a = 57$  Å).

To verify that our systems reduce to classical results of interdiffusion in the long-time limit, some samples were annealed for times larger than the reptation time. Figure 3 shows a plot of the diffusion coefficient  $D$  divided by the self-diffusion coefficient  $D^*$  at 120 °C of PS of  $M_w = 233000$ . It is assumed that  $D$  can be derived from the square halfwidth from the expression

$$\sigma^2 = 4Dt \quad (5)$$

which is valid in the reptation limit—as well as in the case of the conventional diffusion. Figure 3 shows that  $D/D^*$  is a function of time, varying rapidly for short times but

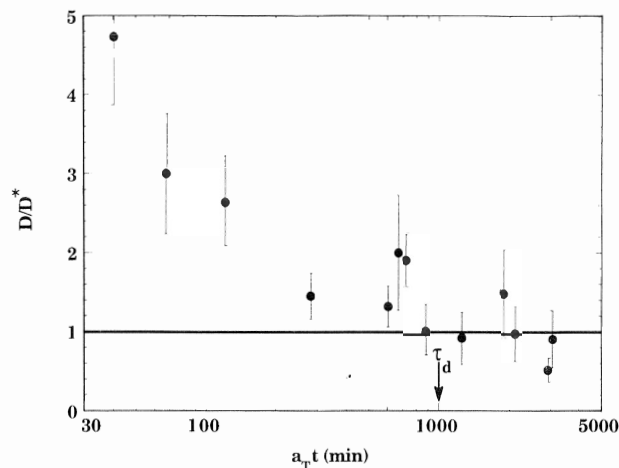


FIG. 3. The diffusion coefficient  $D$  measured from the reflectivity data divided by the self-diffusion coefficient  $D^*$  of PS ( $M_w = 233000$ ) in the bulk at 120 °C as a function of reduced time  $a^2 t$ . For  $t \geq \tau_d$ ,  $D = D^*$ .

then reaching a value of 1 in proximity of the reptation time.<sup>2</sup> This is in full agreement with the body of experimental<sup>3,5,6</sup> and theoretical knowledge<sup>2,15</sup> already obtained for  $t > \tau_d$ . It is worthwhile then to examine how our data fit the predictions made for shorter times.

According to Edwards and Doi,<sup>2</sup> the segmental displacement for a polymer chain reptating in a melt can be approximated by power laws of time within the bounds of the different characteristic relaxation times. Precisely, the mean-square displacement of a chain segment  $\phi(t) = \langle [\mathbf{R}(t) - \mathbf{R}(0)]^2 \rangle$  takes the expressions

$$\frac{6Nb^2}{a} \left( \frac{D^* t}{\pi} \right)^{1/2}, \quad \text{for } t < \tau_e, \quad (6a)$$

$$\left[ 2aNb^2 \left( \frac{D^* t}{\pi} \right)^{1/2} \right]^{1/2}, \quad \text{for } \tau_e < t < \tau_R, \quad (6b)$$

$$(6Nb^2 D^* t)^{1/2}, \quad \text{for } \tau_R < t < \tau_d, \quad (6c)$$

$$6D^* t, \quad \text{for } t > \tau_d. \quad (6d)$$

Comparison of Eq. (6d) with (5) shows that the three-dimensional mean-square displacement of a chain segment is closely related to the mean-square width of the interface:  $\sigma^2 = \frac{2}{3} \phi(t)$ . The calculated values of  $\sigma$  are shown in Fig. 2 as dashed lines, starting at the value of  $\tau$  for which its analytical form is proposed, and continued up to the next relaxation time limit. For  $t > \tau_e$ , the diffusion gradually evolves from segmental motion constrained by entanglements to the motion of the entire molecule. For  $t < \tau_e$ , the width of the interface seems to have relaxed much more rapidly than predicted for the mean displacements of a chain segment, Eq. (6a). This is also in disagreement with the recent molecular-dynamics simulation<sup>8</sup> and spin-echo experiments<sup>7</sup> in bulk polymers. At these short times the diffusion at an interface between two layers might be different from that of the single molecule in the bulk. The causes of it are under examination: either some bias was introduced by joining two separately prepared surfaces, or the conformation of molecules near

the surface are different from the bulk due to chain distortion, number of entanglements, or distribution of chain ends.<sup>16,17</sup>

In conclusion, for  $t > \tau_e$ , the interdiffusion of two polymer layers is in agreement with the power laws predicted from reptation arguments if in the theory the Rouse motion between entanglements is included. At least one of the ansatz of the reptation model is established:  $\tau_d$  is the characteristic time after which the diffusion becomes conventional. Further refinements of the neutron-reflection technique will reduce the scatter in the data points,

making possible a more detailed test of the numerical coefficients as well as of the power exponents. It will also be possible to explore in detail how the different diffusion regimes evolve into each other, and compare such findings with those obtained by computer simulation.<sup>8</sup>

The authors would like to thank Professor E. J. Kramer and S. K. Kumar for several enlightening discussions. The work at Argonne was supported by the U.S. Department of Energy, Basic Energy Sciences, under Contract No. W-31-104-ENG-38.

---

<sup>1</sup>P. G. de Gennes, *Scaling Concepts in Polymer Physics* (Cornell Univ. Press, Ithaca, NY, 1979).

<sup>2</sup>S. F. Edwards and M. Doi, *The Theory of Polymer Dynamics* (Oxford Science, Oxford, 1986).

<sup>3</sup>P. F. Green, Ph.D. thesis, Cornell University, 1985 (unpublished).

<sup>4</sup>P. F. Green and E. J. Kramer, *J. Mater. Res.* **1**, 202 (1986).

<sup>5</sup>J. Klein and B. J. Briscoe, *Proc. R. Soc. London, Ser. A* **365**, 53 (1979).

<sup>6</sup>S. J. Whitlow and R. P. Wool, *Macromolecules* **22**, 2648 (1989).

<sup>7</sup>D. Richter, B. Farago, L. J. Fetters, J. S. Huang, B. Ewen, and C. Lartigue, *Phys. Rev. Lett.* **64**, 1389 (1990).

<sup>8</sup>K. Kremer, G. S. Grest, and I. Carmesin, *Phys. Rev. Lett.* **61**, 566 (1988).

<sup>9</sup>T. P. Russell, A. Karim, A. Mansour, and G. P. Felcher, *Macromolecules* **21**, 1890 (1988).

<sup>10</sup>M. L. Williams, R. F. Landel, and J. D. Ferry, *J. Am. Chem. Soc.* **77**, 3701 (1955).

<sup>11</sup>J. F. Tassin, L. Monnerie, and J. L. Fetters, *Macromolecules* **21**, 240 (1988).

<sup>12</sup>A. Karim, A. Mansour, G. P. Felcher, and T. P. Russell, in *Polymer Based Molecular Composites*, edited by D. W. Schaefer and J. E. Mark, MRS Symposia Proceedings No. 171 (Materials Research Society, Pittsburgh, 1990).

<sup>13</sup>W. W. Graessley, *Adv. Polym. Sci.* **1**, 16 (1974).

<sup>14</sup>J. F. Tassin and L. Monnerie, *Macromolecules* **21**, 1946 (1988).

<sup>15</sup>J. Crank, *The Mathematics of Diffusion*, 2nd ed. (Clarendon, Oxford, 1983).

<sup>16</sup>S. K. Kumar, M. Vacatello, and D. Y. Yoon, *J. Chem. Phys.* **89**, 5206 (1988).

<sup>17</sup>W. G. Madden, *J. Chem. Phys.* **87**, 1405 (1987).